

# Pion exchange interaction in the $\gamma p \rightarrow pe^+e^-$ reaction

Swapn Das <sup>1</sup>

*Nuclear Physics Division, Bhabha Atomic Research Centre,  
Trombay, Mumbai-400085, India*

*Homi Bhabha National Institute, Anushakti Nagar, Mumbai-400094, India*

## Abstract

The  $\rho^0 - \omega$  interference has been studied in the dilepton invariant mass distribution spectra in the photonuclear reaction, but that is not done for the gamma-nucleon reaction. Recent past, the  $e^+e^-$  invariant mass distribution spectrum in the  $\gamma p$  reaction, i.e.,  $\gamma p \rightarrow pe^+e^-$  reaction, was measured at Jefferson Laboratory to look for the  $\rho^0 - \omega$  interference in the multi-GeV region. To study the mechanism of this reaction, the differential cross section of the  $e^+e^-$  invariant mass distribution is calculated in the quoted energy region. The reaction is assumed to proceed as  $\gamma p \rightarrow Vp$ ;  $V \rightarrow e^+e^-$ , where  $V$  denotes a vector meson, i.e., either  $\rho^0$  or  $\omega$  meson. The photoproduction of the vector meson is described by the Vector Meson Dominance (VMD) model which consists of diagonal and off-diagonal processes. The diagonal process is described as  $\gamma \rightarrow V$ ;  $Vp \rightarrow Vp$ . The low energy  $\omega$  meson photoproduction data is well described by the off-diagonal process which is illustrated as  $\gamma \rightarrow \rho^0$ ;  $\rho^0 p \rightarrow \omega p$ . The reaction  $\rho^0 p \rightarrow \omega p$  proceeds due to one pion exchange interaction. The differential cross sections of the  $\gamma p \rightarrow pe^+e^-$  reaction due to the above processes of VMD model are compared, and the significance of the pion exchange interaction is investigated in the energy region of  $\gamma$  beam available at Jefferson Laboratory.

Keywords: Pion exchange interaction, vector meson dominance model,  $\gamma p$  reaction  
PACS number(s): 13.60.-r, 13.60.Le, 13.20.-v

## 1 Introduction

The quantum interference of the  $\rho^0$  and  $\omega$  mesons occurs because of the small difference between the masses of these mesons. This interference is seen in the decay channels of the above mesons which are produced in the nuclear and particle reactions in the multi-GeV region [1]. The  $\rho^0$  meson is preferably identified by the dipion production since it dominantly ( $\sim 100\%$ ) decays as  $\rho^0 \rightarrow \pi^+\pi^-$  [2]. Though the branching ratio of  $\omega \rightarrow \pi^+\pi^-$  is very small compared to that of  $\rho^0$  meson, the  $\rho - \omega$  interference is visible in the  $\pi^+\pi^-$  production in the  $e^+e^-$  [3] (see the references there in) and  $\gamma$  induced [4] reactions. The

---

<sup>1</sup>email: swapand@barc.gov.in

quoted interference is shown to occur in the semihadronic decay channel, i.e.,  $\rho^0, \omega \rightarrow \pi^0 \gamma$ , in the photonuclear reaction [5].

The distinct  $\rho - \omega$  interference has been reported in the dilepton  $e^+e^-$  production in the photonuclear reaction by Alvensleben et al., [6] and Biggs et al., [7]. That was not studied in the photonucleon reaction, only the information about it exists near the threshold region [8]. Recent past, the  $e^+e^-$  invariant mass distribution spectrum in the  $\gamma p$  reaction (i.e.,  $\gamma p \rightarrow pe^+e^-$  reaction) was measured at Jefferson Laboratory (JLab) to the search the  $\rho - \omega$  interference using Bremsstrahlung photon beam of energy range 1.2 to 5.4 GeV. The preliminary results are reported in Ref. [9].

The  $\gamma p \rightarrow pe^+e^-$  reaction is assumed to proceed as  $\gamma p \rightarrow Vp$ ;  $V \rightarrow e^+e^-$ , where  $V$  denotes the vector meson, i.e., either  $\rho^0$  or  $\omega$  meson. The photoproduction of these mesons can be described by the vector meson dominance (VMD) model [1]. According to that, a physical photon is composed of bare photon  $\gamma_B$  and its hadronic component  $\gamma_V$ , i.e.,

$$|\gamma\rangle \simeq \left[ 1 - \sum_{V=\rho^0, \omega, \phi, \dots} \frac{\pi \alpha_{em}}{2\gamma_{\gamma V}^2} \right] |\gamma_B\rangle + \sum_{V=\rho^0, \omega, \phi, \dots} \frac{\sqrt{\pi \alpha_{em}}}{\gamma_{\gamma V}} |\gamma_V\rangle, \quad (1)$$

where  $\alpha_{em}(= 1/137.04)$  is the fine structure constant.  $\gamma_{\gamma V}$  is the photon to vector meson coupling constant [10]. The values of  $\gamma_{\gamma\rho}$  and  $\gamma_{\gamma\omega}$  (as extracted from the measured width of  $\rho^0, \omega \rightarrow e^+e^-$  [11]) are 2.48 and 8.53 respectively [12]. Since the cross section is calculated in the pole mass region of the  $\rho$  and  $\omega$  mesons, other vector mesons (e.g.,  $\phi$  meson) are not considered in the present context.

The hadron production in the nuclear and particle reactions occurs in the GeV region. Since the strength of the electromagnetic interaction is much less ( $\sim 10^{-2}$ ) than that of the hadronic interaction, the first term in Eq. (1) can be neglected in the quoted energy region. The latter, i.e.,  $\gamma_V$ , appears as vector meson  $V$  (e.g.,  $\rho^0$ ,  $\omega$ , ... etc.) due to the photon nucleon (or nucleus) scattering in the GeV region. This mechanism is illustrated by the diagonal and off-diagonal processes of the vector meson dominance (VMD) model. According to the diagonal process, the hadronic part of the photon, i.e.,  $\gamma_V$  in Eq. (1), converts to virtual  $V$  meson followed by the elastic scattering, i.e.,  $\gamma \rightarrow V$ ;  $Vp \rightarrow Vp$ . The coherent contribution of  $\rho^0$  and  $\omega$  mesons, and the  $\rho^0 - \omega$  interference can be described by this process. The off-diagonal process should not be considered for this purpose, since the  $\rho$  meson photoproduction in the off-diagonal process can be ignored as it is negligibly small compared to the diagonal one [1]. This is also true for the  $\omega$  meson photoproduction at high energy [1, 12]. As illustrated by Sibirstev et al. [12], the low energy  $\omega$  meson photoproduction data is better understood by the off-diagonal process, i.e.,  $\gamma \rightarrow \rho^0$ ;  $\rho^0 p \rightarrow \omega p$ . More precisely, the reaction  $\rho^0 p \rightarrow \omega p$  proceeds due to one pion exchange (OPE) interaction [1, 13], i.e., the  $\omega$  meson photoproduction in the off-diagonal process arises because of the pion exchange interaction. The superscripts “ $D$ ” and “ $O$ ” are used

afterwards to differentiate the vector meson production due to diagonal and off-diagonal processes of VMD model respectively.

The differential cross section  $\frac{d\sigma}{dm}$  of the  $e^+e^-$  invariant mass  $m$  distribution in the  $\gamma p \rightarrow pe^+e^-$  reaction is calculated in the multi-GeV region using both diagonal and off-diagonal processes of VMD model. The interference of these processes cannot exist [1], since the previous process involves natural parity exchange whereas the latter (because of OPE interaction) occurs due to unnatural parity exchange. Therefore, the total differential cross section  $\frac{d\sigma}{dm}$  of the above reaction can be written as

$$\frac{d\sigma}{dm} = \frac{d\sigma^D}{dm} + \frac{d\sigma^O}{dm}, \quad (2)$$

where  $\frac{d\sigma^D}{dm}$  represents the differential cross section of the  $\gamma p \rightarrow Vp$ ;  $V \rightarrow e^+e^-$  reaction due to the diagonal process, and  $\frac{d\sigma^O}{dm}$  denotes that of the  $\gamma p \rightarrow \omega p$ ;  $\omega \rightarrow e^+e^-$  reaction due to off-diagonal process of VMD model.

## 2 Formalism

The production of  $V$ (vector) meson in the  $\gamma p \rightarrow Vp$  reaction is described by the production amplitude  $\Pi_{\gamma p \rightarrow Vp}(\mathbf{r})$ , i.e.,

$$\Pi_{\gamma p \rightarrow Vp}(\mathbf{r}) = K f_{\gamma p \rightarrow Vp}(q^2 = 0) \delta(\mathbf{r}); \quad (3)$$

$K = -4\pi(1 + E_V/E_{p'})$  [14, 15].  $E_{p'}$  is the energy of proton in the final state.  $f_{\gamma p \rightarrow Vp}(q^2 = 0)$  denotes the forward amplitude of the  $\gamma p \rightarrow Vp$  reaction in the  $\gamma p$  cm system.  $q^2$  is the four-momentum transfer from the projectile.  $\delta(\mathbf{r})$  is the density distribution of proton (point particle).

The vector meson produced in the  $\gamma p$  reaction propagates in the free space before it decays into  $e^+e^-$ . The propagator of this meson is given by  $(-g_\nu^\mu + \frac{1}{m^2}k_V^\mu k_{V,\nu})G_{0V}(m)$  [14]. The scalar part of it, i.e.,  $G_{0V}(m)$ , can be written as

$$G_{0V}(m) = \frac{1}{m^2 - m_V^2 + im_V \Gamma_V(m)}, \quad (4)$$

where  $m$  is the vector meson mass, i.e.,  $e^+e^-$  invariant mass.  $m_V$  is the pole mass of the meson:  $m_{\rho^0} = 775.26$  MeV and  $m_\omega = 782.65$  MeV, as listed in Ref. [11]. The total decay width of the vector meson  $\Gamma_V(m)$  is composed of the partial widths of various decay channels [11]:  $\Gamma_{\rho^0}(m) = 99.93\% \Gamma_{\rho^0 \rightarrow \pi^+\pi^-}(m) + 0.06\% \Gamma_{\rho^0 \rightarrow \pi^0\gamma}(m) + 0.01\% \Gamma_{\rho^0 \rightarrow e^+e^-}(m)$ , and  $\Gamma_\omega(m) = 89.9\% \Gamma_{\omega \rightarrow \pi^+\pi^-\pi^0}(m) + 8.28\% \Gamma_{\omega \rightarrow \pi^0\gamma}(m) + 1.53\% \Gamma_{\omega \rightarrow \pi^+\pi^-}(m) + 0.29\% \Gamma_{\omega \rightarrow e^+e^-}(m)$ .

The partial decay widths are illustrated in Ref. [16] except the dielectron decay width, i.e.,  $\Gamma_{V \rightarrow e^+e^-}(m)$ , which is given by [12]

$$\Gamma_{V \rightarrow e^+e^-}(m) \simeq \frac{\pi}{3} \left( \frac{\alpha_{em}}{\gamma_{\gamma V}} \right)^2 m. \quad (5)$$

The differential cross section  $\frac{d\sigma}{dm}$  for the dilepton invariant mass  $m$  distribution in the  $(\gamma, V \rightarrow e^+e^-)$  reaction on proton can be written as

$$\frac{d\sigma}{dm} = \int d\Omega_V P_{e^+e^-} \left| \sum_{V=\rho^0, \omega} \Gamma_{V \rightarrow e^+e^-}^{1/2}(m) F_{\gamma, V} \right|^2; \quad (6)$$

$F_{\gamma, V} = G_V(m) K f_{\gamma p \rightarrow V p}(q^2 = 0)$ .  $\Omega_V$  is the solid angle subtended by the vector meson momentum  $\mathbf{k}_V$ . The factor  $P_{e^+e^-}$  arises because of the phase space of the reaction:  $P_{e^+e^-} = \frac{3}{8(2\pi)^3} \frac{k_V^2 m^2}{m_p k_\gamma |k_V E_i - k_\gamma \cos\theta_V E_V|}$ .  $P_{e^+e^-}$  and  $\Omega_V$  are same for both  $\rho^0$  and  $\omega$  mesons.

$\frac{d\sigma}{dm}$  in Eq. (6) has been calculated using the vector meson photoproduction amplitude  $f_{\gamma N \rightarrow V N}$ . Both diagonal and off-diagonal processes of the vector meson dominance (VMD) model relates  $f_{\gamma N \rightarrow V N}$  to the vector meson nucleon scattering amplitude  $f_{V' N \rightarrow V N}$  [12] as

$$f_{\gamma N \rightarrow V N} = \sum_{V'=\rho^0, \omega, \dots} \frac{\sqrt{\pi \alpha_{em}}}{\gamma_{\gamma V'}} f_{V' N \rightarrow V N}, \quad (7)$$

where the constants  $\alpha_{em}$  and  $\gamma_{\gamma V'}$  are defined in Eq. (1).  $\gamma_{\gamma V'}$  for the  $\omega$  meson, i.e.,  $\gamma_{\gamma \omega}$ , is  $\sim 3.5$  times larger than  $\gamma_{\gamma \rho}$ . Therefore, the photoproduction amplitude of the  $\rho^0$  meson can be described well by the diagonal process [1], i.e.,  $f_{\gamma N \rightarrow \rho^0 N} \approx f_{\gamma N \rightarrow \rho^0 N}^D = \frac{\sqrt{\pi \alpha_{em}}}{\gamma_{\gamma \rho}} f_{\rho^0 N \rightarrow \rho^0 N}$ . The  $\rho^0$  meson nucleon scattering amplitude  $f_{\rho^0 N \rightarrow \rho^0 N}$  (extracted from the elementary  $\rho^0$  meson photoproduction data) is taken from the calculation of Kondratyuk et al., [17].

The  $\omega$  meson production in the  $\gamma p \rightarrow \omega p$  reaction, as mentioned earlier, is illustrated by both diagonal and off-diagonal processes of VMD model. Therefore, the amplitude of this reaction, according to Eq. (7), is  $f_{\gamma N \rightarrow \omega N} = f_{\gamma N \rightarrow \omega N}^D + f_{\gamma N \rightarrow \omega N}^O$ , where  $f_{\gamma N \rightarrow \omega N}^D = \frac{\sqrt{\pi \alpha_{em}}}{\gamma_{\gamma \omega}} f_{\omega N \rightarrow \omega N}$  (diagonal process) and  $f_{\gamma N \rightarrow \omega N}^O = \frac{\sqrt{\pi \alpha_{em}}}{\gamma_{\gamma \rho}} f_{\rho^0 N \rightarrow \omega N}$  (off-diagonal process). The energy dependent differential cross section of the previous process [1] is given by

$$\frac{d\sigma^D}{dq^2}(\gamma p \rightarrow \omega p)|_{q^2=0} = C \left( 1 + \frac{D}{E_\gamma} \right); \quad (8)$$

$C = 9.3 \mu\text{b}/\text{GeV}^2$  and  $D = 1.4 \text{ GeV}$ . According to VMD model [12, 18], it can be written as

$$\frac{d\sigma^D}{dq^2}(\gamma p \rightarrow \omega p)|_{q^2=0} = \frac{\alpha_{em}}{16\gamma_{\gamma \omega}^2} \left( \frac{\tilde{k}_\omega}{\tilde{k}_\gamma} \right)^2 [1 + \alpha_{\omega N}^2](\sigma_t^{\omega N})^2, \quad (9)$$

where  $\tilde{k}_\omega$  and  $\tilde{k}_\gamma$  are the c.m. momenta in the  $\omega N$  and  $\gamma N$  systems respectively, evaluated at the c.m. energy of  $\gamma N$  system.  $\alpha_{\omega N}$  is the ratio of the real to imaginary part of the  $\omega N$  scattering amplitude, taken from Ref. [19].  $\sigma_t^{\omega N}$  is the total  $\omega N$  scattering cross section. Using Eqs. (7)-(9), the energy dependent values of the  $\omega$  meson photoproduction amplitude  $f_{\gamma p \rightarrow \omega p}^D$  has been evaluated.

Friman et al., [13] have calculated the total cross section  $\sigma_t^O$  and the differential cross section for the four-momentum transfer distribution  $\frac{d\sigma^O}{dq^2}$  of the  $\gamma p \rightarrow \omega p$  reaction using the off-diagonal process of VMD model, i.e.,  $\gamma \rightarrow \rho^0$ ;  $\rho^0 p \rightarrow \omega p$ . They have used one pion exchange interaction to describe the  $\rho^0 p \rightarrow \omega p$  reaction. The calculated results due to them reproduced well the data of both  $\sigma_t^O$  and  $\frac{d\sigma^O}{dq^2}$  at low energy. Therefore,  $\frac{d\sigma^O}{dq^2}(\gamma p \rightarrow \omega p)$  calculated by Friman et al. [13] is used to extract  $f_{\gamma p \rightarrow \omega p}^O(q^2 = 0)$ . As illustrated by Sibirtsev et al. [12], the forward photoproduction cross section  $\frac{d\sigma}{dq^2}|_{q^2=0}$  of the  $\gamma p \rightarrow \omega p$  reaction is determined through the extrapolation of  $\frac{d\sigma}{dq^2}$  to  $q^2 = 0$ . This extrapolation is done over a range of  $q^2$  (close to  $q^2 = 0$ , e.g.,  $q^2 = -0.01$  to  $-0.03$  GeV<sup>2</sup>) where a fit of the form  $\frac{d\sigma}{dq^2} = \frac{d\sigma}{dq^2}|_{q^2=0} \exp(bq^2)$  can be used. Due to this reason,  $\frac{d\sigma}{dq^2}|_{q^2=0}$  does not vanish at low energy where the differential cross section is clearly dominated by one pion exchange interaction. The magnitude of  $f_{\gamma p \rightarrow \omega p}^O(q^2 = 0)$  is evaluated using the relation [12]:

$$\frac{d\sigma^O}{dq^2}(\gamma p \rightarrow \omega p)|_{q^2=0} = \frac{\pi}{k_\gamma^2} |f_{\gamma p \rightarrow \omega p}^O(q^2 = 0)|^2. \quad (10)$$

In fact,  $|f_{\gamma p \rightarrow \omega p}^O(q^2 = 0)|^2$  is required to calculate the cross section  $\frac{d\sigma^O}{dm}$  in Eq. (6).

### 3 Result and Discussions

Using Eq. (6), the total cross section of the  $\gamma p \rightarrow \omega p$ ;  $\omega \rightarrow e^+e^-$  reaction, i.e.,  $\sigma_t = \int (\frac{d\sigma}{dm}) dm$ , is calculated. For the diagonal process,  $\sigma_t^D$  is calculated using  $f_{\gamma p \rightarrow \omega p}^D$  described in Eq. (9) whereas that due to off-diagonal process (i.e.,  $\sigma_t^O$ ) is worked out using  $f_{\gamma p \rightarrow \omega p}^O$  in Eq. (10). The calculated results are compared in Fig. 1 for the beam energy  $E_\gamma$  range 1.5 – 10 GeV.  $\sigma_t^D$  is shown by the dot-dashed curve which increases significantly with beam energy upto  $E_\gamma = 4$  GeV. Beyond that,  $\sigma_t^D$  increases (with  $E_\gamma$ ) very slowly.  $\sigma_t^O$  (presented by the dot-dot-dashed curve) falls with  $E_\gamma$ . This figure distinctly shows that  $\sigma_t^O$  is significantly larger than  $\sigma_t^D$  at low energy, i.e.,  $E_\gamma < 4$  GeV. For the exclusive  $\omega$  meson production in the intermediate state of the  $\gamma p \rightarrow p e^+ e^-$  reaction,  $\sigma_t^D$  increases and  $\sigma_t^O$  decreases with the increase in the beam energy. Fig. 1 shows that both diagonal and off-diagonal processes are significant for the  $\omega$  meson photoproduction reaction around the beam energy  $E_\gamma = 4$  GeV.  $\sigma_t^D$  is distinctly dominant over  $\sigma_t^O$  at  $E_\gamma \simeq 10$  GeV.

As mentioned earlier, the diagonal process of VMD model describes the production of both  $\rho^0$  and  $\omega$  mesons in the  $\gamma p$  reaction. Therefore, the photoproduction amplitudes of these mesons, i.e.,  $f_{\gamma p \rightarrow \rho^0 p}^D$  and  $f_{\gamma p \rightarrow \omega p}^D$ , due to the above process are added coherently to evaluate the differential cross section for the dielectron mass  $m$  distribution (i.e.,  $\frac{d\sigma^D}{dm}$ ) of the  $\gamma p \rightarrow Vp$ ;  $V \rightarrow e^+e^-$  reaction. The calculated results for  $\frac{d\sigma^D}{dm}$  at  $E_\gamma = 1.5$  GeV are shown in Fig. 2(a). The short-dashed curve represents  $\frac{d\sigma^D}{dm}$  (calculated using  $f_{\gamma p \rightarrow \rho^0 p}^D$ ) occurring due to  $\rho^0$  meson. The broad distribution of this curve arises because of the large width ( $\sim 150$  MeV) of the  $\rho^0$  meson. The narrow distribution shown by the dot-dashed curve (peaking at the  $\omega$  meson pole mass, i.e.,  $\sim 782$  MeV) denotes  $\frac{d\sigma^D}{dm}$  (calculated using  $f_{\gamma p \rightarrow \omega p}^D$ ) because of the  $\omega$  meson. The dotted curve (showing sharp peak at  $\sim 782$  MeV) originates due to the  $\rho - \omega$  interference. Unless mentioned explicitly,  $\frac{d\sigma^D}{dm}$  represents the cross section due to the coherent contribution of  $\rho^0$  and  $\omega$  mesons. It is illustrated by the large-dashed curve, which shows narrow peak at the  $\omega$  meson mass  $\sim 782$  and broad base because of the large width of the  $\rho$  meson. As shown in this figure, the cross section is increased considerably (i.e., by a factor  $\approx 2$ ) due to the  $\rho - \omega$  interference.

In Fig. 2(b), the differential cross sections  $\frac{d\sigma^D}{dm}(\gamma p \rightarrow Vp; V \rightarrow e^+e^-)$  (large-dashed curve) and  $\frac{d\sigma^O}{dm}(\gamma p \rightarrow \omega p; \omega \rightarrow e^+e^-)$  (dot-dot-dashed curve) are compared at  $E_\gamma = 1.5$  GeV. The previous is illustrated in Fig. 2(a). Since the latter describes only the  $\omega$  meson production, it shows narrow distribution peaking at  $\sim 782$  MeV. This figure illustrates that  $\frac{d\sigma^O}{dm}$  is significantly larger than  $\frac{d\sigma^D}{dm}$ , though the latter (as described in Fig. 2(a)) is remarkably increased because of the  $\rho - \omega$  interference. The  $e^+e^-$  emission in the  $\gamma p$  reaction dominantly occurs due to the decay of  $\omega$  meson produced (in the intermediate state) because of the off-diagonal process of VMD model. The total differential cross section  $\frac{d\sigma}{dm}$ , i.e.,  $\frac{d\sigma^D}{dm} + \frac{d\sigma^O}{dm}$  in Eq. (2), is described by the solid curve in Fig. 2(b). It shows the feature similar to other curves appearing in the figure.

The differential cross sections of the  $\gamma p \rightarrow pe^+e^-$  reaction calculated at  $E_\gamma = 3$  GeV are shown in Fig. 3. Various curves appearing in this figure (and all other figures presented afterwards) illustrate those as stated in Fig. 2. The calculated results shown in Fig. 3(a) is qualitatively similar to those in Fig. 2(a). Unlike to that in Fig. 2(b), Fig. 3(b) distinctly shows that  $\frac{d\sigma^D}{dm}$  supersedes  $\frac{d\sigma^O}{dm}$  because of the  $\rho - \omega$  interference.  $\frac{d\sigma^D}{dm}$  increases and  $\frac{d\sigma^O}{dm}$  decreases with the increase in the beam energy. The latter (i.e.,  $\frac{d\sigma^O}{dm}$ ) is significantly large at 3 GeV, as the total differential cross section  $\frac{d\sigma}{dm}$  in Eq. (2) is increased by  $\sim 60\%$  due to it. The calculated results (not presented) show that the enhancement in  $\frac{d\sigma}{dm}$  because of  $\frac{d\sigma^O}{dm}$  is  $\sim 25\%$  at 5 GeV.

To look for the above features at higher energy, the differential cross sections  $\frac{d\sigma^D}{dm}$  and  $\frac{d\sigma^O}{dm}$  are calculated at  $E_\gamma$  taken equal to 10 GeV, and those are presented in Fig. 4. The enhancement in the cross section due to  $\rho - \omega$  interference is distinctly visible in

Fig. 4(a). Unlike to those in Figs. 2(b) and 3(b), Fig. 4(b) shows that  $\frac{d\sigma^O}{dm}$  is negligibly small compared to  $\frac{d\sigma^D}{dm}$ , i.e., the differential cross section  $\frac{d\sigma}{dm}$  in Eq. (2) is increased only 6.7% due to  $\frac{d\sigma^O}{dm}$  at this energy. Therefore, the dilepton  $e^+e^-$  emission in the  $\gamma p$  reaction at  $E_\gamma = 10$  GeV can be described well by the diagonal process of VMD model.

The calculated results illustrate that the  $\gamma p \rightarrow pe^+e^-$  reaction at the fixed photon beam energy in the region  $E_\gamma > 1.5$  GeV to  $E_\gamma \sim 5$  GeV occurs due to both diagonal and off-diagonal processes of VMD model. Since the latter process (as mentioned earlier) arises due to one pion exchange interaction, it is significant in the quoted energy region. At  $E_\gamma \sim 10$  GeV, the considered reaction can be accounted well by the diagonal process which does not involve the pion exchange interaction. Therefore, this interaction around 10 GeV is insignificant for the considered reaction.

The dilepton invariant mass distribution in the  $\gamma p \rightarrow pe^+e^-$  reaction was measured at JLab using Bremsstrahlung photon beam which possesses a certain range of energy. The Bremsstrahlung cross section  $\sigma_B$  varies as  $\frac{1}{E_\gamma}$  [20]. Therefore, the differential cross section  $\frac{d\sigma}{dm}$  of the  $e^+e^-$  invariant mass  $m$  distribution in the Bremsstrahlung beam induced  $\gamma p \rightarrow pe^+e^-$  reaction [21] can be written as

$$\frac{d\sigma}{dm} = \int_{E_{\gamma, mn}}^{E_{\gamma, mx}} dE_\gamma W(E_\gamma) \frac{d\sigma}{dm}(E_\gamma), \quad (11)$$

with  $W(E_\gamma) \propto \frac{1}{E_\gamma}$ . In this equation,  $\frac{d\sigma}{dm}(E_\gamma)$  denotes the differential cross section at the fixed beam energy, given in Eq. (6).  $E_{\gamma, mn}$  and  $E_{\gamma, mx}$  are the minimum and maximum energies respectively of the Bremsstrahlung photon beam.

The differential cross section of the  $\gamma p \rightarrow pe^+e^-$  reaction has been calculated using Eq. (11) for the Bremsstrahlung photon beam energy range  $E_{\gamma, mn} = 1.2$  GeV to  $E_{\gamma, mx} = 5.4$  GeV. This is the energy range used for the measurement done at Jlab, and the preliminary results (as mentioned earlier) are reported in Ref. [9]. The calculated results are presented in Fig. 5, and various curves appearing in it are described in Fig. 2. Fig. 5(a) shows  $\frac{d\sigma^D}{dm}$  in the considered energy range is significantly increased due to  $\rho - \omega$  interference. Both cross sections  $\frac{d\sigma^D}{dm}$  and  $\frac{d\sigma^O}{dm}$ , as illustrated in Fig. 5(b), are significantly large for the quoted reaction, i.e., the cross section  $\frac{d\sigma}{dm}$  ( $= \frac{d\sigma^D}{dm} + \frac{d\sigma^O}{dm}$  in Eq. (2)) is increased by  $\sim 72\%$  because of  $\frac{d\sigma^O}{dm}$ .

The upgrade accelerator facility at JLab can provide electron beam of energy 12 GeV. Therefore, the upper limit of the energy of Bremsstrahlung photon beam can be considered  $\sim 10$  GeV. Bremsstrahlung cross section  $\sigma_B$  at this energy is much less than that at 5.4 GeV because it falls as  $\frac{1}{E_\gamma}$  (mentioned above). As shown in Fig. 4(b), the differential cross section  $\frac{d\sigma^O}{dm}$  of the  $\gamma p \rightarrow pe^+e^-$  reaction is negligibly small (compared to  $\frac{d\sigma^D}{dm}$ ) at  $E_\gamma = 10$  GeV. Both  $\sigma_B$  ( $\propto \frac{1}{E_\gamma}$ ) and  $\frac{d\sigma^O}{dm}$  (see Fig. 2(b)) at  $E_\gamma \ll 10$  GeV are much larger than

those at 10 GeV. Since the energy of Bremsstrahlung photon beam possesses a certain range, the differential cross sections are calculated to search the contribution of  $\frac{d\sigma^O}{dm}$  to  $\frac{d\sigma}{dm}$  for the beam energy range  $E_{\gamma, mn} = 1.2$  GeV to  $E_{\gamma, mx} = 10$  GeV. The calculated results presented in Fig. 6 show that they are qualitatively similar to those depicted in Fig. 5. The figure 6(b) shows that  $\frac{d\sigma^O}{dm}$  in the quoted energy range is considerably large as  $\frac{d\sigma}{dm}$  is increased by  $\sim 43\%$  due to it. Therefore, the pion exchange interaction is significant for the reactions illustrated in Figs. 5 and 6.

## 4 Conclusions

The dielectron emission in the  $\gamma p$  reaction has been studied in the multi-GeV region using the vector meson dominance (VMD) model. The  $e^+e^-$  in the final state is assumed to arise because of the decay of the vector meson  $V$  (i.e., either  $\rho^0$  and  $\omega$  mesons) produced in the intermediate state, i.e.,  $\gamma p \rightarrow Vp$ ;  $V \rightarrow e^+e^-$ . The photoproduction of both  $\rho^0$  and  $\omega$  mesons has been described by the diagonal process of VMD model (i.e.,  $\gamma \rightarrow V$ ;  $Vp \rightarrow Vp$ ). Therefore, the  $\rho - \omega$  interference occurs in this process. The  $\omega$  meson is also photoproduced due to off-diagonal process of VMD model, i.e.,  $\gamma \rightarrow \rho^0$ ;  $\rho^0 p \rightarrow \omega p$ . The reaction  $\rho^0 p \rightarrow \omega p$  proceeds because of one pion exchange interaction, i.e., the off-diagonal process arises due to this interaction. The interference between the diagonal and off-diagonal processes cannot exist.

The calculated results show that the cross section of the  $\gamma p \rightarrow pe^+e^-$  reaction due to the diagonal process ( $\frac{d\sigma^D}{dm}$ ) increases whereas that due to off-diagonal process ( $\frac{d\sigma^O}{dm}$ ) decreases with the increase in the beam energy. In the region  $E_\gamma > 1.5$  GeV to  $E_\gamma \sim 5$  GeV, the considered reaction occurs because of both diagonal and off-diagonal processes. Therefore, the pion exchange interaction is significant in this region. At higher energy (i.e.,  $E_\gamma \sim 10$  GeV),  $\frac{d\sigma^O}{dm}$  is negligibly small compared to  $\frac{d\sigma^D}{dm}$ , i.e., the pion exchange interaction is insignificant around this energy.

For Bremsstrahlung photon beam of minimum energy  $E_{\gamma, mn} = 1.2$  GeV,  $\frac{d\sigma^O}{dm}$  of the  $\gamma p \rightarrow pe^+e^-$  reaction is found considerably large irrespective of the maximum beam energy  $E_{\gamma, mx}$  taken equal to 5.4 or 10 GeV. Therefore, the pion exchange interaction is significant for the Bremsstrahlung beam induced  $\gamma p \rightarrow pe^+e^-$  reaction in the above energy regions.

## 5 Acknowledgement

The author thanks the anonymous referee for the comments which helped to improve the quality of the paper.



## References

- [1] T. H. Bauer, R. D. Spital, D. R. Yennie and F. M. Pipkin, *Rev. Mod. Phys.* **50** (1978) 261; Erratum, *ibid*, **51** (1979) 407.
- [2] H.-J. Behrend et al., *Phys. Rev. Lett.* **24** (1970) 336; H. Alvensleben et al., *Nucl. Phys. B* **18** (1970) 333.
- [3] H. B. O'Connell, B. C. Pearce, A. W. Thomas and A. G. Williams, *Prog. Part. Nucl. Phys.* **39** (1997) 201.
- [4] P. J. Biggs et al., *Phys. Rev. Lett.* **24** (1970) 1201; H.-J. Behrend et al., *Phys. Rev. Lett.* **27** (1971) 61; H. Alvensleben et al., *Phys. Rev. Lett.* **27** (1971) 888.
- [5] Swapan Das, *Phys. Rev. C* **94** (2016) 025204.
- [6] H. Alvensleben et al., *Phys. Rev. Lett.* **25** (1970) 1373.
- [7] P. J. Biggs et al., *Phys. Rev. Lett.* **24** (1970) 1197.
- [8] M. F. M. Lutz and M. Soyeur, *Nucl. Phys. A* **760** (2005) 85.
- [9] C. Djalali et al., *Proceeding of Science (Hadron 2013)* 176.
- [10] J. J. Sakurai, *Currents and Mesons* (The University of Chicago Press, Chicago, 1969); R. K. Bhaduri, *Models of the Nucleon* (Addison-Wesley Publishing Company, Inc., California, 1988).
- [11] K. A. Olive et al., (Particle Data Group), *Chin. Phys. C* **38** (2014) 090001.
- [12] A. Sibirtsev, H.-W. Hammer, U.-G. Meißner and A. W. Thomas, *Eur. Phys. J. A* **29** (2006) 209; A. Sibirtsev, H.-W. Hammer and U.-G. Meißner, *Eur. Phys. J. A* **37** (2008) 287.
- [13] B. Friman and M. Soyeur *Nucl. Phys. A* **600** (1996) 477.
- [14] S. Das, *Eur. Phys. J. A* **49** (2013) 123; *Pramana* **75** (2010) 665.
- [15] A. Pautz and G. Shaw, *Phys. Rev. C* **57** (1998) 2648.
- [16] S. Das, *Rev. C* **72** (2005) 064619; W. Peters, et al., *Nucl. Phys. A* **632** (1998) 109; S. Das, *Rev. C* **78** (2008) 045210.
- [17] L. A. Kondratyuk, A. Sibirtsev, W. Cassing, Ye. S. Golubeva and M. Effenberger, *Phys. Rev. C* **58** (1998) 1078.

- [18] G. I. Lykasov, W. Cassing, A. Sibirtsev and M. V. Rzjanin, Eur. Phys. J. A **6** (1999) 71.
- [19] A. Sibirtsev, Ch. Elster and J. Speth, arXiv:nucl-th/0203044.
- [20] D. I. Sober, et al., Nucl. Instr. and Meth. A **440** (2000) 263.
- [21] M. Kaskulov, E. Hernandez and E. Oset, Eur. Phys. J. A **31** (2007) 245; S. Das, Phys. Rev. C **83** (2011) 064608.

## Figure Captions

1. (color online). The beam energy dependent total cross sections  $\sigma_t^D$  and  $\sigma_t^O$  of the  $\gamma p \rightarrow \omega p$ ;  $\omega \rightarrow e^+e^-$  reaction. The superscripts “ $D$ ” and “ $O$ ” represent the diagonal and off-diagonal processes of the vector meson dominance (VMD) model respectively (see the detail in the text).
2. (color online). (a)  $\frac{d\sigma^D}{dm}$  calculated at  $E_\gamma = 1.5$  GeV using the diagonal process of VMD model.  $\frac{d\sigma^D}{dm}$  due to  $\rho$  and  $\omega$  mesons are represented by the short-dashed and dot-dashed curves respectively. The dotted curve denotes that because of the  $\rho^0 - \omega$  interference.  $\frac{d\sigma^D}{dm}$  due to the coherence contribution of these mesons is shown by the large-dashed curve. (b)  $\frac{d\sigma^D}{dm}$  and  $\frac{d\sigma^O}{dm}$  are compared. The latter (shown by the dot-dot-dashed curve) is calculated for the  $\omega$  meson produced in the off-diagonal process of VMD model.  $\frac{d\sigma}{dm} = \frac{d\sigma^D}{dm} + \frac{d\sigma^O}{dm}$  is represented by the solid curve in the figure.
3. (color online). Same as those presented in Fig. 2 but for the beam energy  $E_\gamma$  taken equal to 3 GeV.
4. (color online). Same as those illustrated in Fig. 2 but for  $E_\gamma = 10$  GeV.
5. (color online). The curves represent those as described in Fig. 2 but for the Bremsstrahlung photon beam of the energy range:  $E_\gamma = 1.2 - 5.4$  GeV.
6. (color online). Same as those in Fig. 5 but for  $E_\gamma = 1.2 - 10$  GeV.

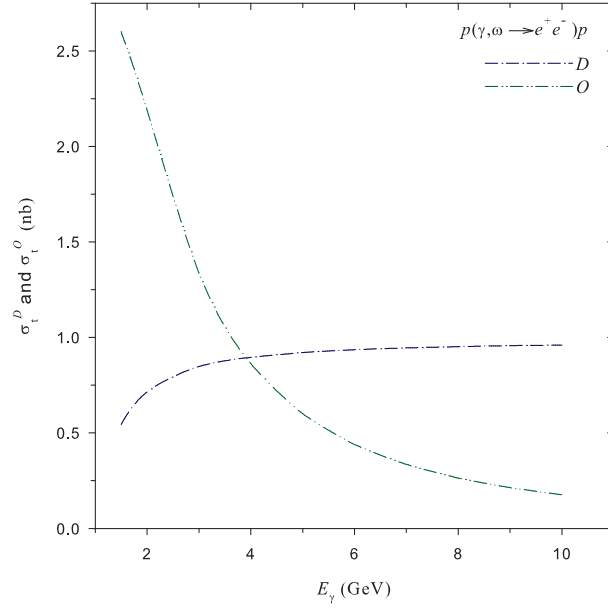


Figure 1: (color online). The beam energy dependent total cross sections  $\sigma_t^D$  and  $\sigma_t^O$  of the  $\gamma p \rightarrow \omega p; \omega \rightarrow e^+e^-$  reaction. The superscripts “ $D$ ” and “ $O$ ” represent the diagonal and off-diagonal processes of the vector meson dominance (VMD) model respectively (see the detail in the text).

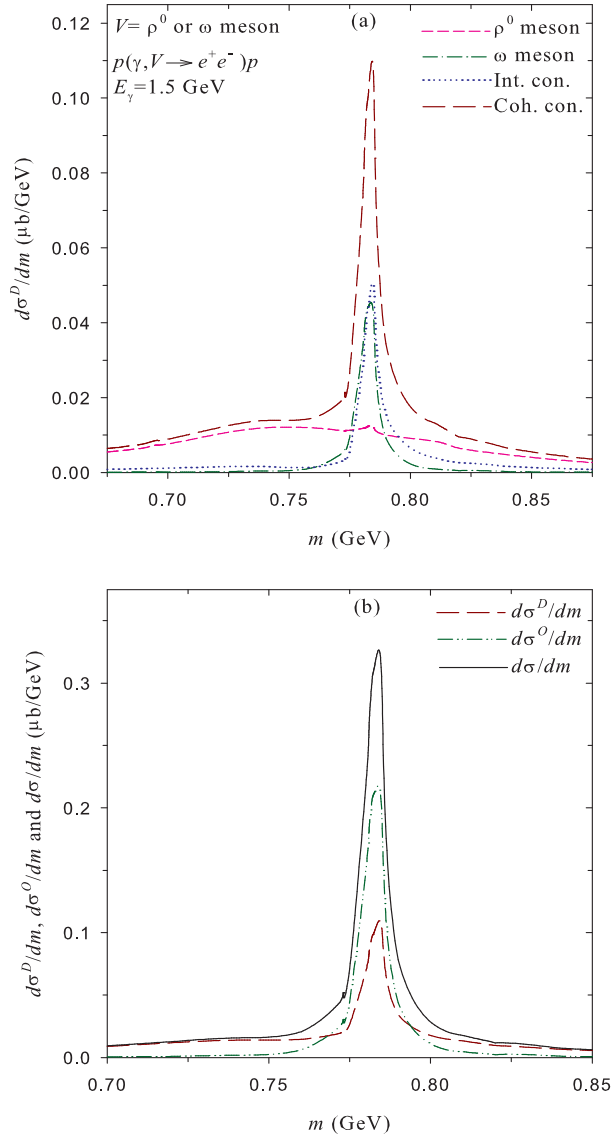


Figure 2: (color online). (a)  $\frac{d\sigma^D}{dm}$  calculated at  $E_\gamma = 1.5$  GeV using the diagonal process of VMD model.  $\frac{d\sigma^D}{dm}$  due to  $\rho$  and  $\omega$  mesons are represented by the short-dashed and dot-dashed curves respectively. The dotted curve denotes that because of the  $\rho^0 - \omega$  interference.  $\frac{d\sigma^D}{dm}$  due to the coherence contribution of these mesons is shown by the large-dashed curve. (b)  $\frac{d\sigma^D}{dm}$  and  $\frac{d\sigma^O}{dm}$  are compared. The latter (shown by the dot-dot-dashed curve) is calculated for the  $\omega$  meson produced in the off-diagonal process of VMD model.  $\frac{d\sigma}{dm} = \frac{d\sigma^D}{dm} + \frac{d\sigma^O}{dm}$  is represented by the solid curve in the figure.

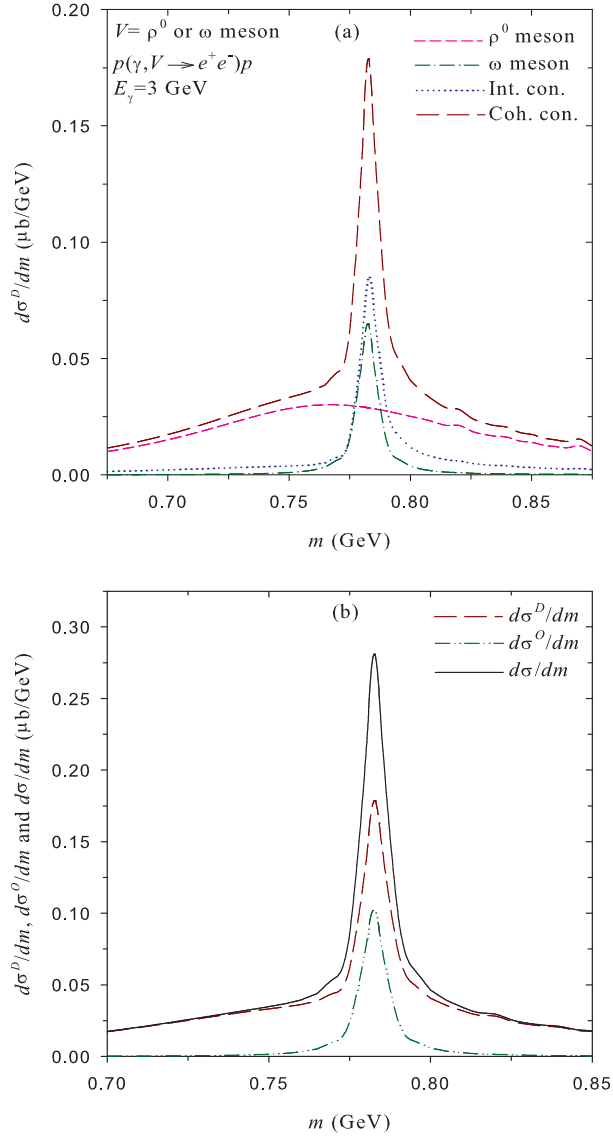


Figure 3: (color online). Same as those presented in Fig. 2 but for the beam energy  $E_\gamma$  taken equal to 3 GeV.

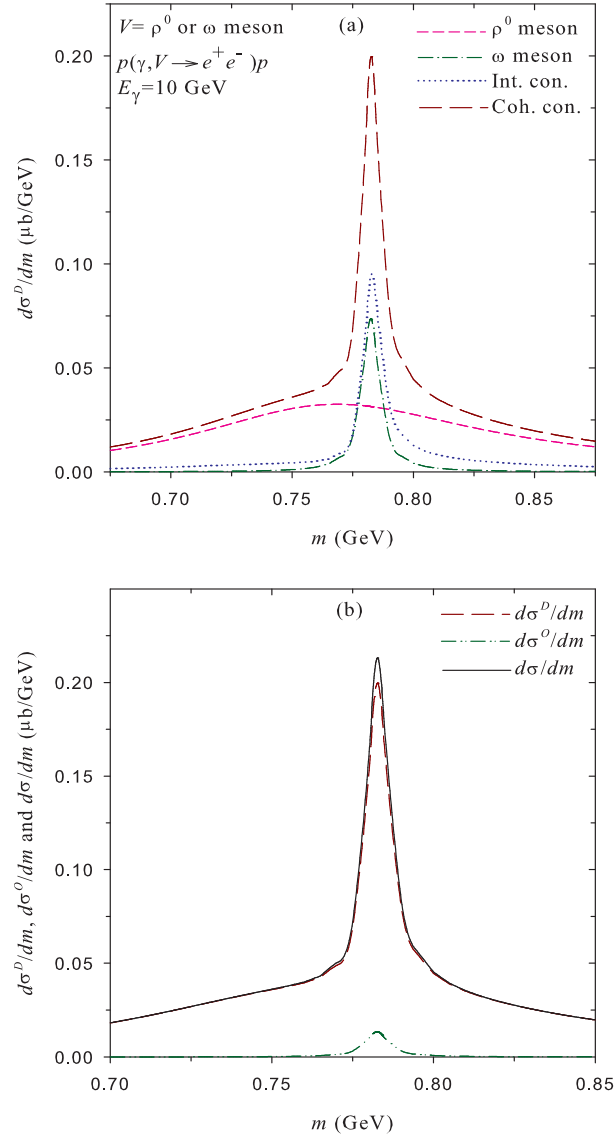


Figure 4: (color online). Same as those illustrated in Fig. 2 but for  $E_\gamma = 10$  GeV.

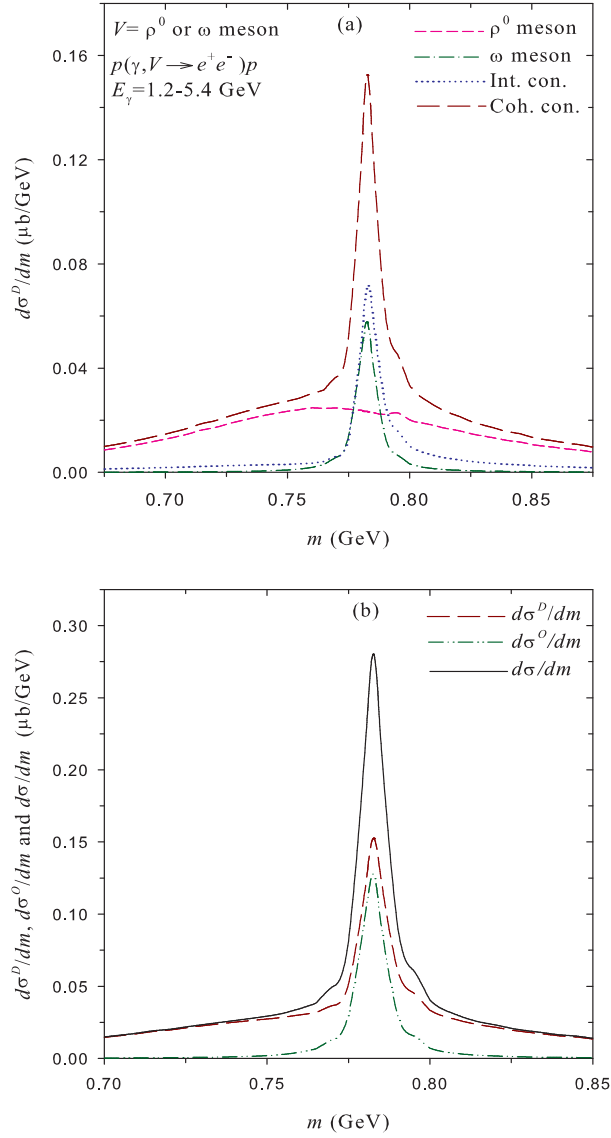


Figure 5: (color online). The curves represent those as described in Fig. 2 but for the Bremsstrahlung photon beam of the energy range:  $E_\gamma = 1.2 - 5.4$  GeV.



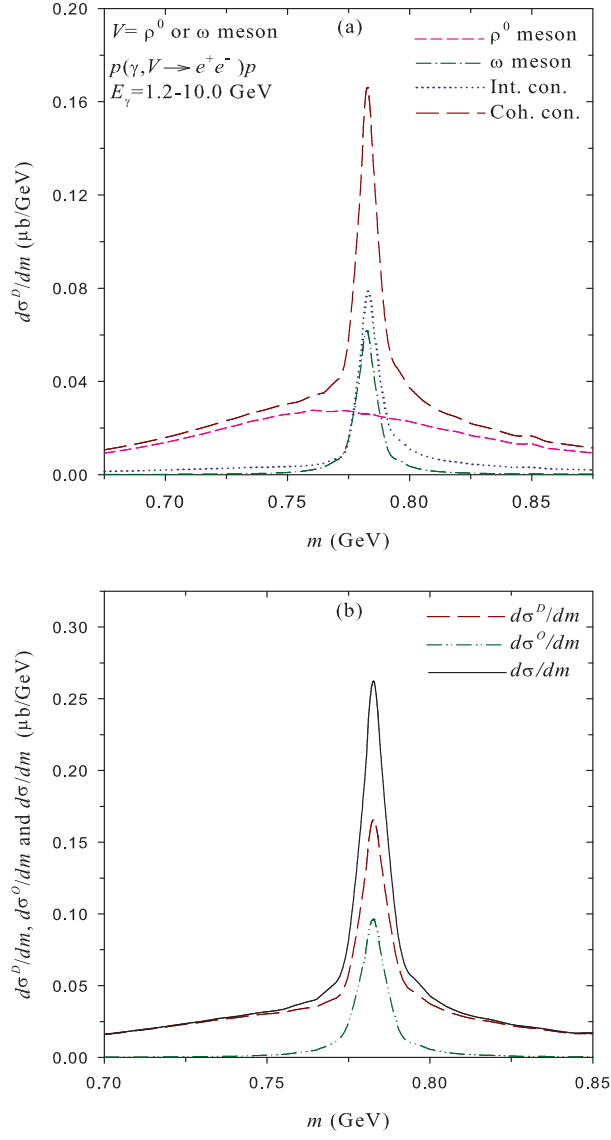


Figure 6: (color online). Same as those in Fig. 5 but for  $E_\gamma = 1.2 - 10$  GeV.